d-wave bipolaronic stripes and two energy scales in cuprates

A.S. Alexandrov

Department of Physics, Loughborough University, Loughborough LE11 3TU, United Kingdom

There is strong experimental evidence for pairing of polaronic carriers in the normal state, two distinct energy scales, d-wave superconducting order parameter, and charge segregation in the form of stripes in several cuprates. All these remarkable phenomena might be unified in the framework of the bipolaron theory as a result of the formation of mobile bipolarons in the normal state and their Bose-Einstein condensation. Extending the BCS theory towards an intermediate and strong-coupling regime we show that there are two energy scales in this regime, a temperature independent incoherent gap and a temperature dependent coherent gap combining into one temperature dependent global gap. The temperature dependence of the gap and single particle (Giaver) tunnelling spectra in cuprates are quantitatively described. A framework for understanding of two distinct energy scales observed in Giaver tunnelling and Andreev reflection experiments is provided. We suggest that both d-wave superconducting order parameter and striped charge distribution result from the bipolaron (center-of-mass) energy band dispersion rather than from any particular interaction.

PACS numbers:74.20.-z,74.65.+n,74.60.Mj

Introduction

There is strong evidence for normal state gaps in high- T_c cuprates from the uniform susceptibility [1,2], inelastic neutron scattering and NMR [3,4], electron energy-loss spectroscopy [5], specific heat [6], angle-resolved photoemission (ARPES) [7,8], tunnelling [9,10], photoexcited quasiparticle relaxation [11], and some kinetic measurements [12]. One view supported by ARPES is that the gap reflects precursor superconducting correlations in the BCS-like state below some characteristic temperature T^* without long range phase coherence. Testing of this hypothesis with specific heat [6] and tunnelling [9] data find that it cannot be sustained. In particular, there is no sign that the gap closes at a given temperature T^* . On the other hand the strong-coupling extension of the BCS theory based on the multi-polaron perturbation technique firmly predicts the transition to a charged Bose liquid in the crossover region of the BCS coupling constant $\lambda \simeq 1$ [13]. (Bi)polaronic nature of carriers in cuprates, supported by the infrared spectroscopy and quite a few other experiments [14], in particular by the isotope effect on the carrier mass [15] provides a natural microscopic explanation of the normal state gap [16]. In the framework of the bipolaron theory the ground state of cuprates is a charged Bose-liquid of intersite mobile bipolarons where single polarons exist as excitations with the energy $\Delta \sim T^*$ or larger [17]. A characteristic temperature T^* of the normal phase is a crossover temperature of the order of Δ where the population of the polaronic band becomes comparable with the bipolaron density. Along this line the normal state kinetics of cuprates has been explained [17] and a theory of tunnelling [18] and angle-resoleved photoemission [19] in cuprates has been developed describing essential spectral features of a single hole in these doped Mott insulators.

However the temperature and doping dependence of the gap still remains a subject of controversy. Moreover, reflection experiments, in which an incoming electron from the normal side of a normal/superconducting contact is reflected as a hole along the same trajectory [20], revealed a much smaller gap edge than the bias at the tunnelling conductance maxima in a few underdoped cuprates [21]. Recent intrinsic tunnelling measurements on a series of Bi '2212' single crystals [22] showed distinctly different behaviour of the superconducting and normal state gaps with the magnetic field. Such coexistance of two distinct gaps in cuprates is not well understood [23,22]. There is also a *d*-like superconducting order parameter (changing sign when the CuO_2 plane is rotated by $\pi/2$ in cuprates as observed in the phasesensitive experiments [24]. And, finally, there is growing experimental evidence [25,26] that stripes occur in doped cuprates. The CuO_2 plane of high-T_c cuprates has been found to be inhomogeneous on the microscopic scale, suggesting that holes condense into large stripe domains [27].

Here I suggest that two distinct energy scales, d-wave superconducting order parameter, and charge segregation in cuprates are manifestations of one and the same phenomenon, which is the normal state pairing of polaronic holes in the doped charge-transfer Mott insulators. The main assumption is that a short-range attraction potential in cuprates is large compared with the (renormalised) polaron Fermi energy. Our main point is independent of the microscopic nature of the attraction. Real-space pairs might be lattice and/or spin bipolarons [17], or any other preformed pairs.

2. Normal and superconducting gap in cuprates

Recently we have proposed a toy model [28], which accounts for two energy scales. The model is a onedimensional Hamiltonian including kinetic energy of carriers in an effective mass (m) approximation and a local attraction potential, $V(x - x') = -U\delta(x - x')$ as

$$H = \sum_{s} \int dx \psi_{s}^{\dagger}(x) \left(-\frac{1}{2m} \frac{d^{2}}{dx^{2}} - \mu \right) \psi_{s}(x) - U \int dx \psi_{\uparrow}^{\dagger}(x) \psi_{\downarrow}^{\dagger}(x) \psi_{\downarrow}(x) \psi_{\uparrow}(x),$$
(1)

where $s = \uparrow, \downarrow$ is the spin ($\hbar = k_B = 1$). The first band to be doped in cuprates is the oxygen band inside the Hubbard gap as established in polarised photoemission [19]. This band is almost one dimensional as discussed in Ref. [18], so that our (quasi) one-dimensional approximation is a realistic starting point. Solving a two-particle problem with the δ -function potential one obtains a bound state with the binding energy $2\Delta_p = \frac{1}{4}mU^2$, and with the radius of the bound state r = 2/mU. We assume that this radius is less than the inter-carrier distance in cuprates, which puts a constraint on the doping level, $E_F < 2\Delta_p$, where E_F is the polaron Fermi energy. Then real-space pairs are formed. If three-dimensional corrections to the energy spectrum of pairs are taken into account (see, for example, Ref. [29]) the ground state of the system is the Bose-Einstein condensate (BEC). The chemical potential is pinned below the band edge by about Δ_p both in the superconducting and normal state [17], so that the normal state single-particle gap is Δ_p .

Two distinct energy scales appear naturally if we take into account that in the superconducting state $(T < T_c)$ the single-particle excitations interact with the condensate via the same potential U. Applying the Bogoliubov approximation [30] we reduce the Hamiltonian, Eq.(1) to a quadratic form as

$$H = \sum_{s} \int dx \psi_{s}^{\dagger}(x) \left(-\frac{1}{2m} \frac{d^{2}}{dx^{2}} - \mu \right) \psi_{s}(x)$$

$$+ \int dx [\Delta_c \psi^{\dagger}_{\uparrow}(x)\psi^{\dagger}_{\downarrow}(x) + H.c.], \qquad (2)$$

where the coherent pairing potential, $\Delta_c = -U\langle \psi_{\downarrow}(x)\psi_{\uparrow}(x)\rangle$, is proportional to the square root of the condensate density, $\Delta_c = constant \times n_0(T)^{1/2}$. The single-particle excitation energy spectrum E(k) is found using the Bogoliubov transformation as

$$E(k) = \left[(k^2/2m + \Delta_p)^2 + \Delta_c^2 \right]^{1/2}.$$
 (3)

This spectrum is quite different from the BCS quasiparticles because the chemical potential is negative with respect to the bottom of the single-particle band, $\mu = -\Delta_p$. The single particle gap, Δ , defined as the minimum of E(k), is given by

$$\Delta = \left[\Delta_p^2 + \Delta_c^2\right]^{1/2}.\tag{4}$$

It varies with temperature from $\Delta(0) = \left[\Delta_p^2 + \Delta_c(0)^2\right]^{1/2}$ at zero temperature down to the temperature independent Δ_p above T_c . The condensate density depends on temperature as $1 - (T/T_c)^{d/2}$ in the ideal three (d = 3) and (quasi) twodimensional (d = 2) Bose-gas. In the three-dimensional charged Bose-gas it has an exponential temperature dependence at low temperatures due to a plasma gap in the Bogoliubov excitation spectrum [31], which might be highly anisotropic in cuprates [17]. Near T_c one can expect a power law dependence, $n_0(T) \propto 1 - (T/T_c)^n$ with n > d/2 because the condensate plasmon [31] depends on temperature. As shown in Ref. [28] the theoretical temperature dependence, Eq.(4) describes well the pioneering experimental observation of the anomalous gap in $YBa_2Cu_3O_{7-\delta}$ in the electron-energy-loss spectra by Demuth et al [5], with $\Delta_c(T)^2 = \Delta_c(0)^2 \times [1 - (T/T_c)^n]$ below T_c and zero above T_c , and n = 4.

3. Giaver tunnelling and Andreev reflection

The normal metal-superconductor (SIN) tunnelling conductance via a dielectric contact, dI/dV is proportional to the density of states, $\rho(E)$ of the spectrum Eq.(3). Taking also into account the scattering of single-particle excitations by a random potential, thermal lattice and spin fluctuations as described in Ref. [18] one finds at T = 0

$$dI/dV \propto \left[\rho\left(\frac{2eV - 2\Delta}{\epsilon}\right) + A\rho\left(\frac{-2eV - 2\Delta}{\epsilon}\right)\right],$$
 (5)

with

$$\rho(\xi) = \frac{4}{\pi^2} \times \frac{Ai(-2\xi)Ai'(-2\xi) + Bi(-2\xi)Bi'(-2\xi)}{[Ai(-2\xi)^2 + Bi(-2\xi)^2]^2}, \quad (6)$$

A is the asymmetry coefficient [18], Ai(x), Bi(x) the Airy functions, and ϵ is the scattering rate. We compare the

conductance, Eq.(5) with one of the best STM spectra measured in Ni-substituted $Bi_2Sr_2CaCu_2O_{8+x}$ single crystals by Hancottee *et al* [32], Fig.1a. This experiment showed anomalously large $2\Delta/T_c > 12$.

The theoretical conductance, Eq.(5) describes well the anomalous gap/T_c ratio, injection/emission assymmetry, zero-bias conductance at zero temperature, and the spectral shape inside and outside the gap region. There is no doubt that the gap, Fig.1 is s-like. The conductance, Eq.(5) fits also well the conductance curve obtained on 'pure' Bi2212 single crystals [32], while a simple d-wave BCS density of states cannot describe the excess spectral weight in the peaks and the shape of the conductance outside the gap region. We notice that the scattering rate, ϵ , derived from the fit, is apparently smaller in the 'pure' sample than in Ni- substituted one, as expected.

The same toy model provides a simple theory of tunnelling into bosonic (bipolaronic) superconductor in the metallic (no-barrier) regime [28]. As in the canonical BCS approach applied to the Andreev tunnelling by Blonder, Tinkham and Klapwijk [33], the incoming electron produces only outgoing particles in the superconductor (x > l), allowing for a reflected electron and (Andreev) hole in the normal metal (x < 0). There is also a buffer layer of the thickness l at the normal metalsuperconductor boundary (x = 0), where the chemical potential with respect to the bottom of the conduction band changes gradually from a positive large value μ in the metal to a negative value $-\Delta_p$ in the bosonic superconductor. We approximate this buffer layer by a layer with a constant chemical potential μ_b $(-\Delta_p < \mu_b < \mu)$ and with the same strength of the pairing potential Δ_c as in the bulk superconductor. The Bogoliubov-de Gennes equations may be written as usual [33], with the only difference that the chemical potential with respect to the bottom of the band is a function of the coordinate x,

$$\begin{pmatrix} -(1/2m)d^2/dx^2 - \mu(x) & \Delta_c \\ \Delta_c & (1/2m)d^2/dx^2 + \mu(x) \end{pmatrix} \psi(x) \\ &= E\psi(x) \quad (7)$$

Thus the two-componet wave function in the normal metal is given by

$$\psi_n(x<0) = \begin{pmatrix} 1\\0 \end{pmatrix} e^{iq^+x} + b \begin{pmatrix} 1\\0 \end{pmatrix} e^{-iq^+x} + a \begin{pmatrix} 0\\1 \end{pmatrix} e^{-iq^-x},$$
(8)

while in the buffer layer it has the form

$$\psi_b(0 < x < l) = \alpha \begin{pmatrix} 1 \\ \frac{\Delta_c}{E+\xi} \end{pmatrix} e^{ip^+x} + \beta \begin{pmatrix} 1 \\ \frac{\Delta_c}{E-\xi} \end{pmatrix} e^{-ip^-x} + \gamma \begin{pmatrix} 1 \\ \frac{\Delta_c}{E+\xi} \end{pmatrix} e^{-ip^+x} + \delta \begin{pmatrix} 1 \\ \frac{\Delta_c}{E-\xi} \end{pmatrix} e^{ip^-x}, \quad (9)$$

where the momenta associated with the energy E are $q^{\pm} = [2m(\mu \pm E)]^{1/2}$ and $p^{\pm} = [2m(\mu_b \pm \xi)]^{1/2}$ with

 $\xi = (E^2 - \Delta_c^2)^{1/2}$. The well-behaved solution in the superconductor with negative chemical potential is given by

$$\psi_s(x>l) = c \left(\frac{1}{\frac{\Delta_c}{E+\xi}}\right) e^{ik^+x} + d \left(\frac{1}{\frac{\Delta_c}{E-\xi}}\right) e^{ik^-x}, \quad (10)$$

where the momenta associated with the energy Eare $k^{\pm} = [2m(-\Delta_p \pm \xi)]^{1/2}$. The coefficients $a, b, c, d, \alpha, \beta, \gamma, \delta$ are determined from the boundary conditions, which are continuity of $\psi(x)$ and its first derivative at x = 0 and x = l. Applying the boundary conditions, and carrying out an algebraic reduction, we find

$$a = 2\Delta_c q^+ (p^+ f^- g^+ - p^- f^+ g^-)/D, \qquad (11)$$

$$b = -1 + 2q^{+}[(E + \xi)f^{+}(q^{-}f^{-} - p^{-}g^{-})/D - 2q^{+}(E - \xi)f^{-}(q^{-}f^{+} - p^{+}g^{+})]/D,$$
(12)

with

$$D = (E + \xi)(q^+f^+ + p^+g^+)(q^-f^- - p^-g^-) - (E - \xi)(q^+f^- + p^-g^-)(q^-f^+ - p^+g^+),$$
(13)

and $f^{\pm} = p^{\pm} \cos(p^{\pm}l) - ik^{\pm} \sin(p^{\pm}l), g^{\pm} = k^{\pm} \cos(p^{\pm}l) - ip^{\pm} \sin(p^{\pm}l).$

The transmisson coefficient for electrical current, 1 + $|a|^2 - |b|^2$ is shown in Fig.2 for different values of l when the coherent gap Δ_c is smaller than the pair-breaking gap Δ_p . We find two distinct energy scales, one is Δ_c in the subgap region due to electron-hole reflection and the other one is Δ , which is the single-particle band edge. We notice that the transmission has no subgap structure if the buffer layer is absent (l = 0) in both cases. In the extreme case of a wide buffer layer, $l >> (2m\Delta_p)^{-1/2}$, Fig.2. there are some oscillations of the transmission due to the bound states inside the buffer layer. It was shown in Ref. [35] that the pair-breaking gap Δ_p is inverse proportional to the doping level. On the other hand, the coherent gap Δ_c scales with the condensate density, and therefore with the critical temperature, determined as the Bose-Einstein condensation temperature of strongly anisotropic 3D bosons [29]. Therefore we expect that $\Delta_p >> \Delta_c$ in the underdoped cuprates, Fig.2. Thus the model accounts for the two different gaps experimentally observed in Giaver tunnelling and electron-hole reflection in the underdoped cuprates [23].

One of the important experimental findings is the zerobias conductance peak (ZBCP) observed in a number of in-plane tunnel junctions [34]. Within our approach, ZBCP-like feature appears in the junctions with $\Delta_p > \Delta_c$ and l >> 1 (see thin dashed line in Fig.2). Overdoped cuprates might be in the BCS or intermediate regime because the increasing number of holes leads to an increase of their Fermi energy and, at the same time, to a decrease of Δ_p due to screening [35]. Then, the condition for BEC, $E_F < 2\Delta_p$ no longer holds, and the d-wave BCS approach [36] might account for ZBCP as well. Such evolution from the BEC regime in underdoped cuprates to the BCS-like regime in the overdoped samples has been found in the conserving T-matrix approximation of the two-dimensional attractive Hubbard model [37]. The binding energy of real-space pairs monotonically decreased with increasing density, and vanished at a critical density of holes $n_{cr} = 0.19$ (per cell).

4. D-wave Bose-Einstein condensate

To account for the symmetry of the order parameter and the orientation dependence of ZBCP our simple onedimensional continuos model can be readily extended to two and three dimensions, discrete lattices, and nonlocal pair potential. Than, quite generally, the symmetry of the single-particle spectrum, Eq.(3) and the symmetry of the Bose-Einstein condensate wave-function (i.e. of the order parameter) are not necessary the same in the bosonic superconductor [18]. The single-particle spectrum is dominated by the incoherent (s-wave) gap, Δ_p , in agreement with the c-axis tunnelling data, Fig.1. On the other hand, the symmetry of the Bose-Einstein condensate depends on the bosonic pair (center of mass) energy band dispersion.

Different bipolaron configurations can be found with computer simulation techniques based on the minimization of the ground state energy of an ionic lattice with two holes. The intersite pairing of the in-plane oxygen hole with the *apex* one is energetically favorable in the layered perovskite structures as established by Catlow *et al* [38]. This apex or peroxy-like bipolaron can tunnel from one cell to another via a direct *single polaron* tunnelling from one apex oxygen to its apex neighbor. The bipolaron band structure has been derived in Ref. [39] as

$$E_{\mathbf{k}}^{x,y} = t\cos(k_{x,y}) - t'\cos(k_{y,x}). \tag{14}$$

Here the in-plane lattice constant is taken as a = 1, t is twice the bipolaron hopping integral between p orbitals of the same symmetry elongated in the direction of the hopping $(pp\sigma)$ and -t' is twice the hopping integral in the perpendicular direction $(pp\pi)$. These hopping integrals are proportional to the single-particle hopping integrals between *apex* oxygen ions. The bipolaron energy spectrum in the tight binding approximation consists of two bands $E^{x,y}$ formed by the overlap of p_x and p_y apex polaron orbitals, respectively. The energy band minima are found at the Brillouin zone boundary, $\mathbf{k} = (\pm \pi, 0)$ and $\mathbf{k} = (0, \pm \pi)$ rather than at the Γ point owing to the opposite sign of the $pp\sigma$ and $pp\pi$ hopping integrals. Neither band is invariant under crystal symmetry but the degenerate doublet is an irreducible representation; under a $\pi/2$ rotation the x band transforms into y and vice versa.

If the bipolaron density is low, the bipolaron Hamil-

tonian can be mapped onto the charged Bose-gas [17]. Charged bosons are condensed below T_c into the states of the Brillouin zone with the lowest energy, which are $\mathbf{k} = (\pm \pi, 0)$ and $\mathbf{k} = (0, \pm \pi)$ for the x and y bipolarons, respectively. These four states are degenerate, so the condensate field-operator $\Psi(\mathbf{m})$ in the real (site) space $\mathbf{m} = (m_x, m_y)$ is given by

$$\hat{\Psi}_{\pm}(\mathbf{m}) = N^{-1/2} \sum_{\mathbf{k} = (\pm \pi, 0), (0, \pm \pi)} b_{\mathbf{k}} exp(-i\mathbf{k} \cdot \mathbf{m}).$$
 (15)

where N is the number of cells in the crystal, and $b_{\mathbf{k}}$ is the bipolaron (boson) annihilation operator in \mathbf{k} space. This is a *c*-number below T_c , so that the condensate wave function, which is the superconducting order parameter, is given by

$$\Psi_{\pm}(\mathbf{m}) = n_c^{1/2} \left[\cos(\pi m_x) \pm \cos(\pi m_y) \right], \qquad (16)$$

where n_c is the number of bosons per cell in the condensate. Other combinations of the four degenerate states do not respect time-reversal and (or) parity symmetry. The two solutions, Eq.(16), are physically identical being related by: $\Psi_+(m_x, m_y) = \Psi_-(m_x, m_y + 1)$. They have *d*-wave symmetry changing sign when the CuO_2 plane is rotated by $\pi/2$ around (0,0) for Ψ_- or around (0,1) for Ψ_+ . The *d*-wave symmetry is entirely due to the bipolaron energy dispersion with four minima at $\mathbf{k} \neq \mathbf{0}$.

5. Bipolaronic stripes

The antiferromagnetic interaction are thought to give rise to charge segregation (stripes) in cuprates [40,41]. At the same time the electron-phonon interaction is strong in ionic cuprates and manganites [17,42]. While for wide band polar semiconductors and polymers the charge segregation (strings) were discussed some time ago [43], a role of the long-range Fröhlich electron-phonon interaction in the charge segregation in *narrow* band ionic insulators like cuprates has been addressed only recently [44,45] with the opposite conclusions about existance of strings.

We have proved [45] that the Fröhlich interaction combined with the direct Coulomb repulsion does not lead to charge segregation like strings in doped narrow-band insulators, both in the nonadiabatic and adiabatic regimes. The polarisation potential energy of M fermions trapped in a string of the length N,

$$U = -\frac{e^2}{\kappa} M^2 I_N, \tag{17}$$

appears to be lower in value than the repulsive Coulomb energy because $\kappa = \epsilon_0 \epsilon_\infty / (\epsilon_0 - \epsilon_\infty)$ is always larger than the high-frequency dielectric constant ϵ_∞ . Here ϵ_0 is the static dielectric constant, and the integral I_N is given by

$$I_N = \frac{\pi}{(2\pi)^3} \int_{-\pi}^{\pi} dx \int_{-\pi}^{\pi} dy \int_{-\pi}^{\pi} dz \frac{\sin(Nx/2)^2}{N^2 \sin(x/2)^2} \times (3 - \cos x - \cos y - \cos z)^{-1}.$$
 (18)

It has the following asymptotics at large N

$$I_N = \frac{1.31 + \ln N}{N}.$$
 (19)

The Coulomb energy of spinless one-dimensional fermions comprising both Hartree and exchange terms is [46]

$$E_C = \frac{e^2 M (M-1)}{N \epsilon_{\infty}} [0.916 + \ln M], \qquad (20)$$

so that the polarisation and Coulomb energy per particle becomes

$$U/M = \frac{e^2 M}{N\epsilon_{\infty}} [0.916 + \ln M - \alpha (1.31 + \ln N)], \quad (21)$$

where $\alpha = 1 - \epsilon_{\infty}/\epsilon_0 < 1$. Minimising this energy with respect to the length of the string N we find

$$N = M^{1/\alpha} \exp(-0.31 + 0.916/\alpha), \qquad (22)$$

and

$$(U/M)_{min} = -\frac{e^2}{\kappa} M^{1-1/\alpha} \exp(0.31 - 0.916/\alpha).$$
 (23)

One can see that the potential energy per particle increases with the number of particles. Hence, the energy of M well separated polarons is lower than the energy of polarons trapped in a string no matter correlated or not. The opposite conclusion derived in Ref. [44] originates in an erroneous approximation of the integral $I_N \propto N^{0.15}/N$. The correct asymptotic result is $I_N = \ln(N)/N$.

In principle, the situation might be different if the antiferromagnetic interaction of doped holes with the parent Mott insulator is strong enough [40,41]. Due to the longrange nature of the Coulomb repulsion the length of a single stripe should be finite (see, also Ref. [25,47]). Including the Fröhlich, Eq.(17) and Coulomb Eq.(20) contributions one can readily estimate its length for any type of the short-range *intersite* attraction, E_{att} as [45]

$$N = \exp\left(\frac{\epsilon_0 a E_{att} \delta \omega}{e^2 \omega} - 2.31\right),\tag{24}$$

where ω is the characteristic frequency of bosonic excitations (like magnons) responsible for the short-range attraction, $\delta\omega$ its maximum dispersion, and a is the lattice constant. Then, with typical values of $\epsilon_0 = 30$, a = 3.8Å and $E_{att} = 2J = 0.3$ eV of the t-J model one can hardly expect any charge segregation due to antiferromagnetic spin fluctuations as well, because N < 2 according to Eq.(24). Hence it is more probable that the lattice and spin polarons in cuprates remain in a liquid state in the relevant region of the parameters.

The Fröhlich interaction is not the only electronphonon interaction in ionic solids. As discussed in Ref. [17], any short range electron-phonon interaction, like, for example, the deformation potential and/or Jahn-Teller distortion can overcome the residual weak repulsion of Fröhlich polarons to form small bipolarons. At large distances small bipolarons weakly repel each other due to the long-range Coulomb interaction, strongly suppressed by optical phonons. Hence, they form a liquid state in the relevant region of their densities and masses [48], which is also confirmed by recent study [49] of the Holstein-Hubbard model. The ground state of the 1D Holstein-Hubbard model is a liquid of intersite bipolarons with a significantly reduced mass [49]. The bound states of three or more polarons are not stable.

If (bi)polaronic carriers in cuprates are in the liquid state, one can pose a key question how stripes can be seen at all. Here I suggest that the bipolaron liquid might be striped owing to the bipolaron energy band dispersion, Eq.(14), rather than to any particular interaction. If bipolaron bands have their minima at finite \mathbf{k} (including the Brillouin zone boundaries), then the condensate wave function is modulated in the real space Eq.(16). As a result, the hole density, which is about twice of the condensate density at low temperatures, is striped, with the characteristic period of stripes determined by the inverse band-minima wave vectors. If disorder is strong enough, the condensate might be localised within the wide and shallow random potential wells, so bipolaronic stripes can also exist in the insulating (due to disorder) oxides. If the condensate is striped, one can expect rather different values of the coherent gap, Δ_c , for single-particle excitations tunnelling along (110) and (100), and, hence the different Andreev reflection spectra. Our interpretation of stripes is consistent with recent inelastic neutron scattering studies of YBa₂Cu₃O_{7- δ} [50,51], where the incommensurate peaks in neutron scattering have been only observed in the superconducting state. The vanishing at T_c of the incommensurate peaks can be actually anticipated over a wide part of the phase diagram and in other neutron data [52]. It is, of course, inconsistent with the usual stripe picture where a characteristic distance needs to be observed in the normal state as well. In our picture with the d-wave striped Bose-Einstein condensate the incommensurate neutron peaks disappear at T_c or slightly above T_c (due to superconducting fluctuations), as observed.

To conclude I suggest that two distinct energy scales, d-wave superconducting order parameter and stripes in underdoped cuprates are manifestations of mobile bipolarons. The normal state gap in the charge channel is half of the bipolaron binding energy. The superconducting gap comprises additional coherent part owing to the interaction of single holes with the Bose-Einstein condensate. d-wave superconducting order parameter and stripes are intimately connected as the result of the bipolaron energy band dispersion with the minima at finite wave vectors of the center-of-mass Brillouin zone.

I greatly appreciate enlightening discussions with Antonio Bianconi and Robert Laughlin.

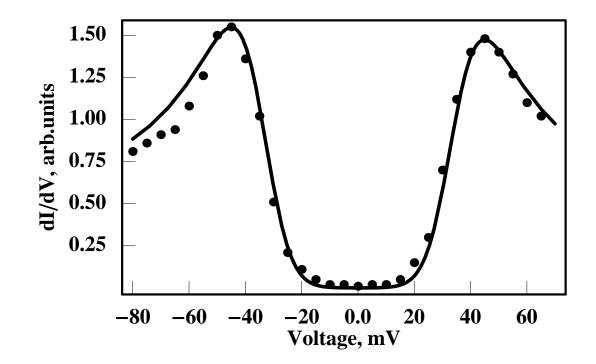
- [1] D.C. Johnston, Phys. Rev. Lett. 62 957 (1989)
- [2] K.A. Müller *et al*, J.Phys.: Condens. Matter **10**, L291 (1998).
- [3] J. Rossat-Mignot *et al*, Physica (Amsterdam) B 18–181, 383 (1992).
- [4] For a comprehensive review see C. Berthier *et al*, J. Phys. I France 6, 2205 (1996).
- [5] J.E. Demuth et al, Phys. Rev. Lett. 64, 603 (1990).
- [6] J.W. Loram et al, J. of Superconductivity 7, 243 (1994).
- [7] Z.-X. Shen and J.R. Schrieffer, Phys. Rev. Lett. 78, 1771 (1997) and references therein.
- [8] N.L. Saini et al, Phys. Rev. Lett. 79, 3467 (1997).
- [9] Ch. Renner *et al*, Phys. Rev. Lett. **80**, 149 (1998).
- [10] A. Mourachkine, Europhys. Lett. **49**, 86 (2000).
- [11] V.V. Kabanov, J. Demsar, B. Podobnik, and D. Mihailovic, Phys. Rev. B 59, 1497 (1999).
- [12] B. Batlogg *et al*, Physica C (Amsterdam) **135-140**, 130 (1994).
- [13] A.S. Alexandrov, Zh.Fiz.Khim. 57, 273 (1983)
 (Russ.J.Phys.Chem.57, 167 (1983)).
- [14] D.B. Tanner and T. Timusk, in 'Physical Properties of High-Temperature Superconductors III', ed. D.M. Ginsberg, World Scientific, Singapore (1992); E.K.H. Salje, A.S. Alexandrov, and W.Y. Liang (eds), 'Polarons and Bipolarons in High-T_c Superconductors and Related Materials', Cambridge University Press, Cambridge (1995), J.T. Devreese, in Encyclopedia of Applied Physics, vol. 14, p. 383, VCH Publishers (1996).
- [15] G. Zhao *et al*, Nature **385**, 236 (1997).
- [16] A.S. Alexandrov, Physica C (Amsterdam) 182, 327 (1991).
- [17] A.S. Alexandrov and N.F. Mott, Rep. Prog. Phys. 57 1197 (1994); *Polarons and Bipolarons*, World-Scientific (1995).
- [18] A.S. Alexandrov, Physica C (Amsterdam) **305**, 46 (1998).
- [19] A.S. Alexandrov and C.J. Dent, Phys. Rev. B60, 15414 (1999).
- [20] A.F. Andreev, Zh. Eksp. Teor. Fiz. 46, 1823 (1964) [Sov. Phys. JETP 19, 1228 (1964)].
- [21] Y. Yagil *et al*, Physica C (Amsterdam) **250**, 59 (1995).
- [22] P. Müller *et al*, unpublished.
- [23] G. Deutscher, Nature **397**, 410 (1999).
- [24] C.C. Tsuei *et al*, Science **272**, 329 (1996) and references therein.
- [25] A. Bianconi, J. Phys. IV France, 9, 325 (1999) and references therein.
- [26] J.M. Tranquada et al, Nature 375, 561 (1996).

- [27] A. Bianconi *et al*, Physica C **296**, 269 (1998).
- [28] A.C. Alexandrov and A.F. Andreev, cond-mat/0005315, to be published.
- [29] A.S. Alexandrov and V.V. Kabanov, Phys. Rev. B 59, 13628 (1999).
- [30] N. Bogoliubov, J.Phys. USSR 11, 23-32(1947).
- [31] L.L. Foldy, Phys.Rev. **124**, 649(1961).
- [32] H. Hancotte et al, Phys. Rev. B55, R3410 (1997).
- [33] G.E. Blonder, M. Tinkham, and T.M. Klapwijk, Phys. Rev. B25, 4515 (1982).
- [34] L. Alff et al, Phys. Rev. B55, R14757 (1997); M. Covington et al, Phys. Rev. Lett. 79, 277 (1997); S. Sinha and K.W. Ng, Phys. Rev. Lett 80, 1296 (1998), W. Wang et al, Phys. Rev. B 60, 4272 (1999) and references therein.
- [35] A.S. Alexandrov, V.V. Kabanov and N.F. Mott, Phys. Rev. Lett. 77, 4796 (1996).
- [36] Y. Tanaka and S. Kashiwaya, Phys. Rev. Lett 74, 3451 (1995).
- [37] B.Kyung, E.G. Klepfish and P.E. Kornilovitch, Phys. rev. Lett. 80, 3109 (1998).
- [38] C.R.A. Catlow, M.S. Islam and X. Zhang, J. Phys.: Condens. Matter 10, L49 (1998).
- [39] A.S. Alexandrov, Phys. Rev. B53, 2863 (1996).
- [40] J. Zaanen and O. Gunnarsson, Phys. Rev. B 40, 7391 (1989).
- [41] V. J. Emery *et al*, Phys. Rev. B 56, 6120 (1997) and references therein.
- [42] A.S. Alexandrov and A.M. Bratkovsky, J. Phys.: Condens. Matter 11, L531 (1999).
- [43] L.N. Grigorov, Makromol. Chem., Macromol. Symp. 37, 159 (1990).
- [44] F.V. Kusmartsev, Phys. Rev. Lett., 84, 530 (2000).
- [45] A.S. Alexandrov and V.V. Kabanov, cond-mat/0005419, to be published.
- [46] This expression differs numerically from Ref. [47].
- [47] F.V. Kusmartsev, J. Phys. IV France, 9, 321 (1999).
- [48] A.S. Alexandrov, Phys. Rev. B **61**, 12315 (2000).
- [49] J. Bonca et al, Phys. Rev. Lett., 84, (2000).
- [50] P. Bourges *et al*, Science **288**, 1234 (2000).
- [51] P. Bourges et al, cond-mat/0006085.
- [52] H.A. Mook *et al*, Nature **395**, 580 (1998); M. Arai *et al*, Phys. Rev. Lett. **83**, 608 (1999); P. Dai *et al*, Phys. Rev. Lett. **80**, 1738 (1998).

Figure Captures

Fig.1. Theoretical tunnelling conductance, Eq.(5) (line) compared with the STM conductance in Nisubstituted $Bi_2Sr_2CaCu_2O_{8+x}$ [32] (dots) with $2\Delta = 90$ meV, A = 1.05, $\epsilon = 40$ meV.

Fig.2. Transmission versus voltage (measured in units of Δ_p/e) for $\Delta_c = 0.2\Delta_p$, $\mu = 10\Delta_p$, $\mu_b = 2\Delta_p$ and l = 0 (thick line), l = 1 (thick dashed line), l = 4 (thin line), and l = 8 (thin dashed line) (in units of $1/(2m\Delta_p)^{1/2}$).



arXiv:cond-mat/0005315 v3 25 May 2000

